Simulating High Reynolds Number Flow by Lattice Boltzmann Method

Simulating High Reynolds Number Flow by Lattice Boltzmann Method *

KANG Xiu-Ying(康秀英)[1], LIU Da-He(刘大禾)[1**], ZHOU Jing(周静)[1], JIN Yong-Juan(金永娟)[2]

[1] *Applied Optics Beijing Area Major Laboratory, Department of Physics, Beijing Normal University, Beijing 100875*
[2] *Institute of Hematology, Chinese Academy of Medical Sciences, Tianjin 300020*

(Received 25 January 2005)

A two-dimensional channel flow with different Reynolds numbers is tested by using the lattice Boltzmann method under different pressure and velocity boundary conditions. The results show that the simulation error increases, and the pressure and the flow rate become unstable under a high Reynolds number. To improve the simulation precision under a high Reynolds number, the number of fluid nodes should be enlarged. For a higher Reynolds-number flow, the velocity boundary with an approximately parabolic velocity profile is found to be more adaptive. Blood flow in an artery with cosine shape symmetrical narrowing is then simulated under a velocity boundary condition. Its velocity, pressure and wall shear stress distributions are consistent with previous studies.

PACS: 47.11.+J, 47.27.Lx, 87.19.Tt

The lattice Boltzmann method (LBM)[1−3] has recently been proven to be competitive for studying flows in various physical systems, such as Newtonian blood flow,[4,5] suspension flow,[6] and complex flow in porous materials.[7] By imposing inlet and outlet boundary conditions, the LBM model, a nonlinear and self-feedback system, may become unstable under a high Reynolds number *Re*. In this study, a two-dimensional channel flow is tested by using the model with different Reynolds numbers under different pressure and velocity boundary conditions, and flow distribution in an artery with cosine shape symmetrical narrowing is then simulated under a velocity boundary condition.

The LBM model is constructed on lattice space that contains fluid particles. Each of these particles is given a discrete set of velocity for travelling from one node on the grid to another. The particles are redistributed on each node according to a set of rules that govern the collision process. Figure 1 shows a nine-velocity square lattice in two dimensions we chose to work on. Let $f_i(\boldsymbol{r},t)$ be a non-negative real number describing the distribution function of the fluid density at node $\boldsymbol{r}$ and time $\boldsymbol{t}$ moving in direction $\boldsymbol{e}_i$. The distribution function evolves the single relaxation-time Bhatnagar–Gross–Krook (BGK) operator according to the Boltzmann equation that is discrete in space-time,

$$f_i(\boldsymbol{r}+\boldsymbol{e}_i\cdot\delta t, t+\delta t) = f_i(\boldsymbol{r},t) + \frac{f_i^{eq}-f_i(\boldsymbol{r},t)}{\tau}, \quad (1)$$

where macroscopic density ρ and velocity $\boldsymbol{u}$ are defined by $\rho = \Sigma f_i$, $\rho\boldsymbol{u} = \Sigma f_i\boldsymbol{e}_i$;

$$\boldsymbol{e}_i = (0,0),\ i=0;$$
$$\Big(\cos\Big[(i-1)\frac{\pi}{2}\Big],\ \sin\Big[(i-1)\frac{\pi}{2}\Big]\Big)c, \quad i=1,2,3,4;$$
$$\Big(\cos\Big[(2i-1)\frac{\pi}{4}\Big],\ \sin\Big[(2i-1)\frac{\pi}{4}\Big]\Big)c, \quad i=5,6,7,8$$

are the nine velocity vectors; $c=\delta\boldsymbol{x}/\delta t$; $\delta\boldsymbol{x}$ and δt are the lattice constant and the time step respectively; τ is the relaxation coefficient; f_i^{eq} is the equilibrium distribution function in direction i related to density ρ and velocity $\boldsymbol{u}=(u_x,u_y)$. For the nine-velocity model, we have

$$f_i^{eq} = \rho\omega_i\Big[1+\frac{3\boldsymbol{e}_i\cdot\boldsymbol{u}}{c^2}+\frac{9}{2}\frac{(\boldsymbol{e}_i\cdot\boldsymbol{u})^2}{c^4}-\frac{3}{2}\frac{\boldsymbol{u}^2}{c^2}\Big], \quad (2)$$

where ω_i is the weighting factor given by $\omega_i = 4/9$, $i=0$; $\omega_i = 1/9$, $i=1,2,3,4$; $\omega_i = 1/36$, $i=5,6,7,8$. The macroscopic continuity equation and the Navier–Stokes equation can be obtained by Taylor expansion of the lattice Boltzmann equation up to $o(\delta t^2)$ and application of a multi-scale Chapman–Enskog procedure,

$$\frac{\partial\rho}{\partial t}+\nabla\cdot(\rho\boldsymbol{u})=0,$$
$$\frac{\partial(\rho\boldsymbol{u})}{\partial t}+\nabla\cdot(\rho\boldsymbol{u}\boldsymbol{u}) = -\nabla p+\nu(\nabla^2(\rho\boldsymbol{u})+\nabla(\nabla\cdot\rho\boldsymbol{u})), \quad (3)$$

where p and ν are the pressure and viscosity defined by $p=c_s^2\rho$, $c_s^2=c^2/3$, and $\nu=(2\tau-1)c^2\delta t/6$, respectively. The stress tensor can be obtained from the non-equilibrium parts of the distribution functions

$$\tau_{\alpha\beta} = -\rho c_s^2\delta_{\alpha\beta}-\Big(1-\frac{1}{2\tau}\Big)\sum_{i=0}^{8}(f_i-f_i^{eq})\boldsymbol{e}_{i\alpha}\cdot\boldsymbol{e}_{i\beta},$$
$$\alpha,\beta=x,y.$$

* Supported by the National Natural Science Foundation of China under Grant No 10274006, and the Ministry of Education of China under Grant No 03011.

** To whom correspondence should be addressed. Email: dhliu@bnu.edu.cn

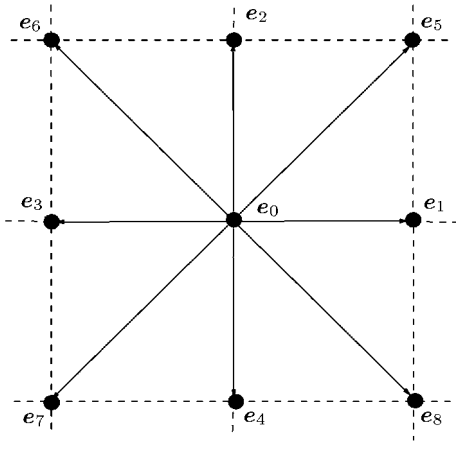

Fig. 1. Basic cell.

In this work, a channel flow of $N_x \times N_y = 64 \times 34$ with x along the channel direction is considered. For a no-slip wall boundary, the halfway bounce-back scheme was used.[3,8] At the inlet and outlet of the channel, pressure and velocity boundary conditions are imposed, respectively. The Reynolds number was defined as $Re = DU/\nu$, where U and D are the maximal velocity and diameter of the tube respectively. The relative error between the simulated and theoretical exact solutions was given by

$$E_{\rm err} = \frac{\{\int_0^D [u_{LBM}(y) - u_{\rm exact}(y)]^2 dy\}^{1/2}}{[\int_0^D u_{\rm exact}^2(y) dy]^{1/2}}, \qquad (4)$$

where $u_{\rm LBM}(y)$ and $u_{\rm exact}(y)$ are the simulated and exact velocity functions of the tube, respectively.

Firstly, we present the results under the pressure boundary conditions proposed by Zou *et al.*[9] at inlet and outlet, using the halfway bounce-back scheme at the walls. The initial distributions are set as the equilibrium functions with uniform velocity $\boldsymbol{u} = 0$ and density $\rho_0 = 1.0$. At the inlet and outlet of the tube, the predetermined values of density are imposed as $\rho_{\rm in} = 1.0$ and $\rho_{\rm out} = 0.9998$, respectively, and $u_y = 0$. After streaming, f_2, f_3, f_4, f_6, and f_7 can be known, then f_1, f_5, and f_8 need to be determined at the inlet by

$$\begin{aligned} &f_1 + f_5 + f_8 = \rho_{\rm in} - (f_0 + f_2 + f_3 + f_4 + f_6 + f_7), \\ &f_1 + f_5 + f_8 = \rho_{in} u_x + (f_3 + f_6 + f_7), \\ &f_5 - f_8 = -f_2 + f_4 - f_6 + f_7, \\ &f_1 = f_1^{eq} + f_3 - f_3^{eq}. \end{aligned} \qquad (5)$$

A similar procedure can be applied to the outlet. By changing the relaxation coefficient τ, the flow distributions in the tube for different Re values are simulated. The dependence of relative error on the Reynolds number is shown in Fig. 2. Moreover, the pressure profile along the tube axis under different Re is illustrated in Fig. 3. The results show that with increase of Re, that is, decrease of τ, the error becomes larger. Moreover, when the parameters are close to the region of instability, the pressure distribution along the axis becomes nonlinear and non-uniform in the transverse direction ($Re = 160$ in Fig. 3), and the simulation has unusually large errors because of nonlinearity and self feedback of the LBM model, and introduction of inlet and outlet boundary conditions. Since compressibility error in the LBM model increases with higher velocity, we then decrease the space step $\delta \boldsymbol{x}$ (keeping densities of the inlet and outlet unchanged), Re increases a little and the instability disappears. Thus, the number of fluid nodes should be enlarged in the simulation of a higher Re flow.

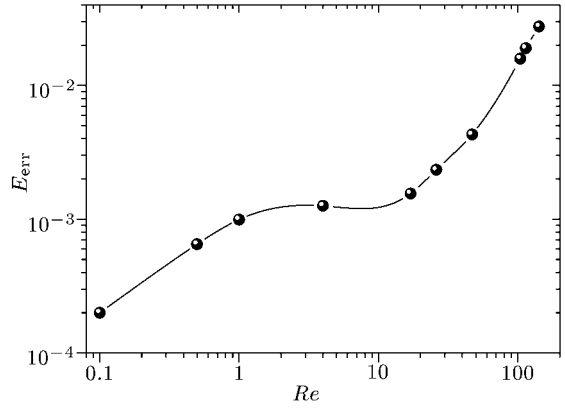

Fig. 2. Dependence of error on Re with a pressure boundary.

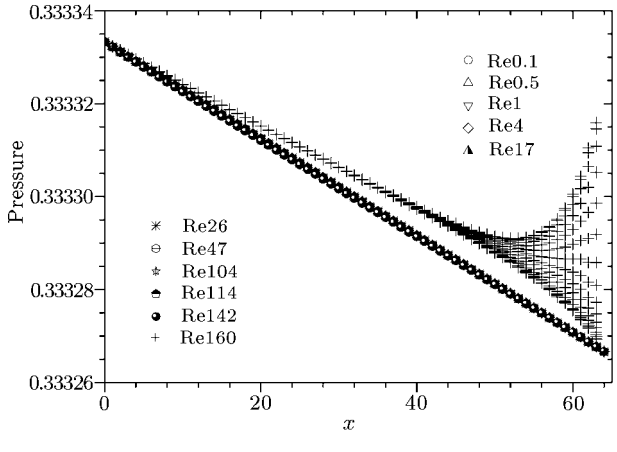

Fig. 3. Pressure distribution along the axis for different Re values.

However, in general applications of the lattice Boltzmann model, the system is usually not a Poiseuille flow. For example, for a stenotic vessel, the pressure gradients at the inlet and outlet are unknown, the length of the simulated tube should increase with the increasing Re value so that the flow at the inlet and outlet are far from the disorder and become

approximately of a Poiseuille distribution. It is interesting in the simulation that a right circular cylinder with diameter ϕ can be positioned in the middle of an initially Poiseuille flow with width $d = 10\phi$. When keeping the pressure gradients unchanged, if the tube length $l = 2d$, the error between the simulated and Poiseuille velocity distributions at the outlet is 0.7%, and the error can reach 22% in the case of $l = 1.5d$. Then, by decreasing τ from 0.53 to 0.52, (i.e. increasing Re), it is found that the error becomes 27% for $l = 2d$, and the error would reduce to 0.4% if $l = 6d$. When τ becomes 0.515, the errors are 3.6% and 0.7% for $l = 6d$ and $l = 8d$, respectively.

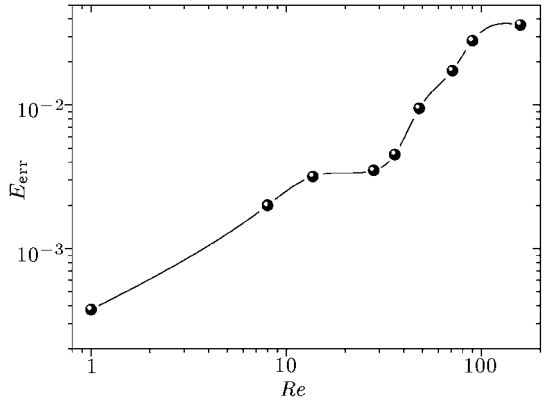

Fig. 4. Dependence of error on Re with velocity boundary.

The next results are presented under velocity boundary conditions at the inlet and outlet by using the halfway bounce-back scheme at the walls. When the tube is long enough, the flow is similar to a Poiseuille flow. At the inlet of the tube, the Fillippova–Hanel curved boundary condition[3,8] with $\Delta = 0.5$ is used. The uniform velocity with $\boldsymbol{u} = 0.01$ is specified along the axial direction at the halfway between the first and second lattices. Moreover, the flow at the outlet is supposed to be fully developed. The equilibrium distribution functions corresponding to the uniform inlet velocity are specified at $t = 0$ throughout the flow field. By changing relaxation coefficient τ, the flow distributions in the tube for different Re are simulated. The exact velocity solution is evaluated by Poiseuille formula with the simulated pressure gradient. The error shown in Fig. 4 also becomes larger with the increasing Re; and by decreasing the space step $\delta\boldsymbol{x}$, the error was reduced and Re increases a little. In fact, to reduce the length of the simulated tube, to minimize the nonlinear effect of the model, and to guarantee the outlet flow developed fully for a higher Re flow, the inlet velocity profile is usually taken to be approximately parabolic distribution. To eliminate the instability, a converged solution for a relatively large value of τ is first used as the initial condition for a smaller value of τ, and then the value of τ decreases gradually so that the converged solutions for the new smaller values of τ can be obtained. Unlike the pressure boundary condition that includes some self-feedback, the flow with higher Re could be simulated by the above velocity boundary. Moreover, it is also observed that the flow rate Q at different cross sections along the axis is non-uniform, as shown in Fig. 5.

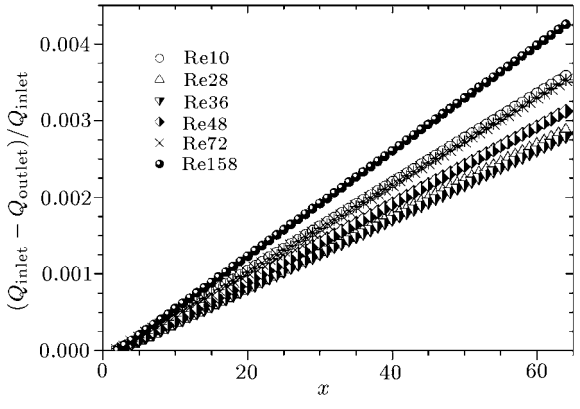

Fig. 5. Relative flow rate along tube axis for different Re.

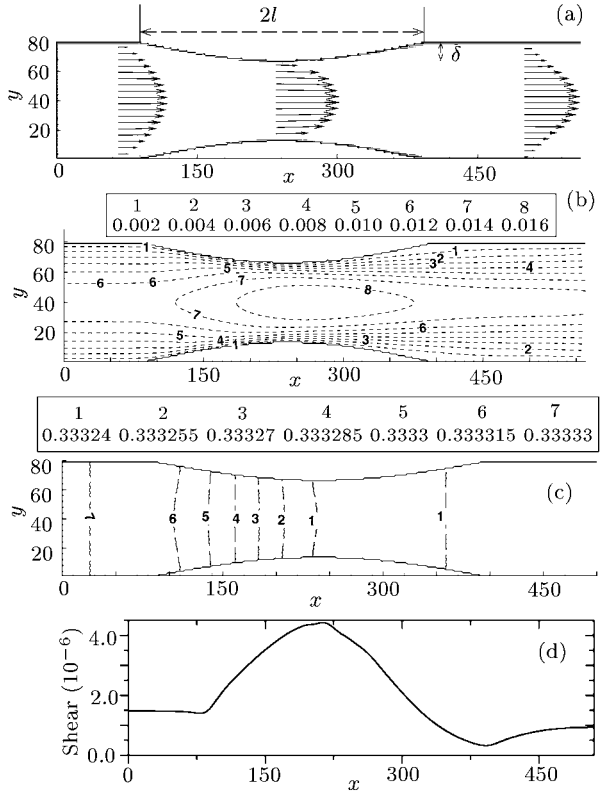

Fig. 6. Stenotic artery flow for $Re = 800$ for a cosine-shaped symmetrical stenosis with $l/\delta = 12.0$ and $\delta = D/6.0$: (a) cross-section velocity profile, (b) velocity contour, (c) pressure contour, (d) wall shear stress.

Then, the flow in a 4-mm diameter artery with

the cosine-shaped symmetrical narrowing is simulated as shown in Fig. 6. At the inlet, the Fillippova–Hanel curved boundary conditions[3,8] is used with $\Delta = 0.5$, such as the above velocity boundary, and its inlet velocity along the vessel axis is only used as a parabolic form with the central maximum velocity u_0. For the vessel walls, the improved Fillippova–Hanel non-slipping curved boundary conditions[3] are used. Moreover, the flow at the outlet is supposed to be fully developed. Blood kinematic viscosity and density are set to be $\nu = 0.0381\,\mathrm{cm}^2/\mathrm{s}$, $\rho = 1.05\,\mathrm{g/cm}^3$, respectively. Currently, many steady flow simulations are carried out with $Re = u_0 D/\nu$ from 100 to 1000, which is in the physiological range for such an artery.[10] The present results show that, in the narrow portion of the tube, the velocity distribution near the centre becomes somehow flatter than the parabolic profile and the mean velocity increases (Figs. 6(a) and 4(b)), and the flowing velocity becomes of a parabolic profile next to the outlet. Moreover, at the narrow portion, the pressure gradient and the wall shear stress become larger (Figs. 6(c) and 6(d)), and the peak of the wall shear stress moves forward with the increasing *Re*, which is in agreement with those reported Refs. [11,12]. When *Re* reaches about 850, the flow cycle appears near the narrowing and becomes wider with the increasing *Re*.

In summary, by introducing inlet and outlet boundary conditions, we have realized that the LBM model for a nonlinear and self-feedback system may become unstable under a higher *Re*. By testing a two-dimensional channel flow under pressure and velocity boundary conditions at the inlet and outlet and halfway bounce-back scheme at the walls, it is shown that the error increases with higher *Re*, the pressure distribution along the axis becomes nonlinear and non-uniform in the transverse direction of the tube and flow rate is non-uniform along the channel under a higher *Re*. To improve the computing precision for high *Re*, the number of fluid nodes should be enlarged. For a high *Re* flow, the velocity boundary with an approximately parabolic profile is more helpful. Moreover, initial distributions of the whole flow should be chosen carefully to eliminate the instability. Flow in an artery with cosine-shaped symmetrical narrowing is simulated using the velocity boundary scheme, and its velocity, pressure and wall shear stress distributions are demonstrated to match with the previous studies.

We are preparing further studies of unsteady flow distribution in arteries with different *Re* and narrowing indexes to show blood flow characters in normal and diseased tubes, which will be helpful to understanding the relationship among the arterial geometric complexity, arterial biomechanics, and arterial wall biology.

Acknowledgments: The authors would like to thank Professor Hai-Ping Fang for suggesting the project and helpful discussion.

References

[1] Qian Y, D'humiéres D and Lallemand P 1992 *Europhys. Lett.* **17** 479
[2] Chen S, Chen H, Matinez D and Matthaeus W 1991 *Phys. Rev. Lett.* **67** 3776
[3] Mei Y, Luo L and Wei S J 1999 *Comput. Phys.* **155** 307
[4] Fang H, Lin Z and Wang Z 1998 *Phys. Rev.* E **57** 25
[5] Fang H, Wang Z, Lin Z and Liu M 2002 *Phys. Rev.* E **65** 051925
[6] Li H, Fang H, Lin Z, Xu S and Chen S 2004 *Phys. Rev.* E **69** 031919
[7] Xu Y, Zhong Y and Huang G 2004 *Chin. Phys. Lett.* **21** 1298
[8] Filippov O and Hanel D 1997 *Comput. Fluids* **26** 697
[9] Zou Q, Hou S, Chen S and Doolen G 1995 *J. Stat. Phys.* **81** 35
[10] Whitmore R L 1968 *Rheology of the Circulation* (Oxford: Pergamon) p 123
[11] John H and Young D 1970 *J. Biom.* **3** 297
[12] Sonu S and Steven H 2003 *J. Biom. Eng.* **125** 445